Cristian V. Ciobanu
e-mail: cciobanu@mines.edu
Division of Engineering,
Colorado School of Mines,
Golden, CO 80401

Adrian Barbu
Department of Computer Science,
University of California,
Los Angeles CA 90095

Ryan M. Briggs
Division of Engineering, Colorado School of
Mines,
Golden, CO 80401

Interactions of Carbon Atoms and Dimer Vacancies on the Si(001) Surface

We investigate the interactions between substitutional carbon atoms on the defect free, (2×1) reconstructed Si(001) surface, and bring evidence that the interaction energy differs significantly from the inverse-cube distance dependence that is predicted by the theory of force dipoles on an elastic half-space. Based on Tersoff potentials, we also calculate the interactions between carbon atoms and dimer vacancies. The calculations indicate that dimer vacancies (DVs) are strongly stabilized by fourth-layer C atoms placed directly underneath them. By use of simple model Monte Carlo simulations, we show that the computed interactions between carbon atoms and DVs lead to self-assembled vacancy lines, in qualitative agreement with recent experimental results. [DOI: 10.1115/1.2019898]

1 Introduction

The alloying of group IV elements (C, Si, Ge) has been pursued as a versatile way to engineer the electronic and structural properties of semiconductor wafers. Independent control of the band gap and of the overall strain has recently been achieved in ternary nanoscale Si-Ge-C systems such as quantum wells and quantum dots, whose design and fabrication are important for the future of high-performance devices that are compatible with current silicon technologies [1,2]. This degree of control was strongly facilitated by the incorporation of carbon into Si and Ge matrices, which has motivated researchers to seek diverse methodologies to achieve this incorporation. Such methodologies include, for instance, metastable growth processes during molecular beam epitaxy [3] and thermal dissociation of acetylene molecules on silicon surfaces [4]. Understanding the physics of carbon incorporation into the substrate during these processes depends, at least in part, on having knowledge of the structure of stable and metastable carbon configurations in the vicinity of the surface. Recent investigations of C_2H_2 dissociation at the surface have provided experimental data needed to make progress in the long-standing problem of finding the atomic configuration of carbon-induced reconstructions [5–10]. In particular, the experiments of Kim et al. [4,11] offer insight into the structure of Si(001) with incorporated carbon. The presence of carbon increases the number of dimer vacancies on the surface for coverages as low as 0.02 monolayers (ML). For carbon coverages up to about 0.05 ML, the dimer vacancies tend to align with one another, giving rise to surface morphologies strikingly similar to the well-known $(2 \times N)$ reconstruction that appears at approximately 1 ML of germanium on Si(001) [12,13]. At even higher carbon coverages (0.06 ML–0.1 ML), the surface displays a $c(4 \times 4)$ structural motif [14]. The similarity between the two markedly different material systems, Si(001) with 1.0 ML of Ge and Si(001) at very low carbon coverage, has prompted us to investigate the mechanism responsible for the self-assembly of vacancy lines on the latter system.

It is thus the purpose of this paper to address the origin of vacancy lines on Si(001) with incorporated carbon atoms. To this end, we compute the interaction energies between carbon atoms and dimer vacancies (DVs) on the Si(001)-(2×1) surface. We have found that the interactions (which are computed here at the level of classical potentials) are able to account for the observed formation of vacancy lines on C/Si(001). Simple Monte Carlo simulations based on the calculated defect interactions show that the thermodynamically stable morphology consists of equidistant, straight vacancy lines. Similar to the Ge/Si(001) system, the separation between the lines is determined by the competition between their (negative) formation energy and their (positive) mutual repulsion. In the limit of small carbon coverages, the main difference from the case of Ge/Si(001) concerns the atomic structure of the lines. As reported in Ref. [4], the C atoms bind to the dimer vacancy by substituting the fourth layer Si atom that lies directly underneath the vacancy (Fig. 1). This structural information enables us to reduce the number of distinct situations in which we compute the interaction energies between carbon atoms and DVs. The numerical procedure for calculating these interactions is outlined in Sec. 2.

In Sec. 3 we report on the interactions between carbon atoms incorporated in the first layer of the defect free Si(001) surface. We find that the interactions of these substitutional atoms are *not* described by the $1/d^3$ distance dependence that is predicted by the elastic theory of force dipoles on a surface. While not entirely unexpected, this result may inspire further investigations into how a given reconstruction of a semiconductor surface influences the interaction of different atomic entities that can be adsorbed on it. Section 4 presents the main results of this article, namely, the interactions between carbon atoms and dimer vacancies. These interactions lead to the formation of carbon-vacancy complexes (CDV) which align in the direction perpendicular to the dimer rows. By studying the surface energy as a function of the distance between the CDV lines, we compute the formation energy of the vacancy lines and their mutual repulsion, and illustrate an energetic mechanism that, under the simplifying hypothesis that kinetic effects can be neglected, explains the self-organization of the vacancy lines. Our conclusions are summarized in Sec. 5.

2 Computational Details

Accurate calculations (at the level of density functional theory) of interactions between point defects on crystal surfaces are very demanding as they require computational slabs that are large in all three dimensions. To cope with the large number of atoms involved, in this work we use empirical potentials to model the interactions between Si and C atoms. We employ the Tersoff potential [15–17], which has become a *de facto* standard for systems such as Si-Ge, Ge, or Si-C. Predictions based on this classical potential have been reported to agree qualitatively with the results of density functional calculations [18,19]. Furthermore, despite
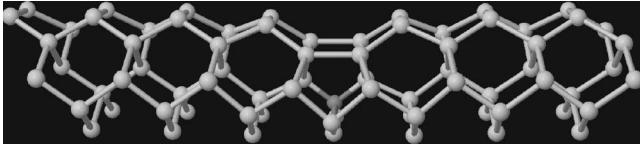
Fig. 1   Atomic structure of a CDV complex on Si(001), with the carbon atom shown in gray

known limitations, this potential has been used with good success for studying the incorporation of C atoms into the Si(001) surface in the high coverage regime (see, e.g., Ref. [10]). It is therefore justifiable to model the atomic interactions with the Tersoff potential [15–17], at least as a starting point for calculating the long-range interactions between defects on Si(001).

We now outline the procedure for determining the interactions between defects, where by defects we understand here carbon atoms (C), dimer vacancies (DV), and carbon-vacancy complexes (CDV). The computational slab used is 24 Å thick, and is subjected to periodic boundary conditions in the plane of the surface. The top part of each slab (≈ 20 Å) is fully relaxed by a conjugate-gradient procedure, while the bottom three layers are kept fixed to simulate the underlying bulk structure. For a defect free Si(001), the surface energy γ_0 of the (2×1) reconstruction is defined by

$$E = N\mu_{Si} + \gamma_0 A, \tag{1}$$

where E is the total energy of the N atoms that are allowed to relax, μ_{Si} is the bulk cohesive energy of silicon, and A is the surface area of the slab. When a DV is created on the surface (see, e.g. [20]), the total energy of the slab can be separated as follows:

$$E = (N-2)\mu_{Si} + \gamma_0 A + u_{DV}, \tag{2}$$

where, in the limit of large dimensions of the simulation slab, the quantity u_{DV} is the formation energy of the dimer vacancy. If a carbon atom is present on the surface, then a similar formula can be used to calculate its formation (incorporation) energy

$$E = N_{Si}\mu_{Si} + N_C\mu_C + \gamma_0 A + u_C, \tag{3}$$

where N_{Si} and N_C ($N_C = 1$) are the numbers of atoms of each type, μ_C is the chemical potential of the C atoms, and u_C is the incorporation energy per atom. Equation (3) also has to be taken in the limit of large in-plane dimensions of the simulation slab; otherwise, the interaction of the periodic images of the substitutional carbon should be accounted for. Such interaction occurs along the dimer row direction, and we can separate it out as a contribution w added to the formation energy u_C

$$E = N_{Si}\mu_{Si} + N_C\mu_C + \gamma_0 A + u_C + w. \tag{4}$$

For two different types of defects (e.g., one dimer vacancy and one C atom), the interaction w can similarly be defined as an excess quantity with respect to the total formation energy ($u_C + u_{DV}$)

$$E = N_{Si}\mu_{Si} + N_C\mu_C + \gamma_0 A + (u_C + u_{DV}) + w, \tag{5}$$

where N_{Si} is the number of Si atoms on the surface after the DV has been formed, and $N_C = 1$. The interaction between two DVs and the interaction between two incorporated carbon atoms are given by formulas similar to Eq. (5), where the numbers of atoms (N_{Si}, N_C) and the formation energies are modified appropriately.

A large number of possible combinations between the types of defects (DV, C), the position of substitutional carbons with respect to the surface, and the in-plane relative positions of these defects can be tabulated. We will, however, focus on the ones that are relevant in the experimental situations described in Refs. [4,11]. Furthermore, we will also report on substitutional C atoms on the defect free Si(001) to illustrate the strong anisotropy effects of the

(2×1) reconstruction on the interactions of carbon atoms incorporated at the surface. Our results are presented and discussed in the next two sections.

3   Interaction of C Atoms on the Defect Free Si(001)

A puzzle in the physics of interacting defects on the Si(001) surface is the distance dependence of the interactions between same-row dimer vacancies, whose long-range repulsion varies as $w \propto d^{-2}$ with their separation d. Evidence for this inverse-square dependence has been provided both by experiments [21–23] and theory [24–26]. The implied reason behind this deviation from the expected d^{-3} behavior [27] is the surface reconstruction. While a deeper investigation as to how exactly a general, reconstructed surface affects the interactions of defects is left for future studies, we report here another remarkable example of deviation from the expected d^{-3} behavior which we have found for carbon atoms substituting silicon on the surface dimers.

Using Eq. (4), we extract the interaction w of substitutional carbon atoms in equivalent positions in the first layer and same dimer row as follows. For a range of distances d between $8a$ and $25a$ [$a = 3.84$ Å is the dimer spacing on Si(001)-(2×1)], we fit the excess energy $\Delta E \equiv E - N_{Si}\mu_{Si} - \gamma_0 A$ to the simple functional form

$$\Delta E = B + \beta(d/a)^{-p}, \tag{6}$$

where B, β, and p are fitting constants. Since the interaction of the substitutional defects vanishes in the large d limit, from Eqs. (3) and (4) we identify the parameter B as the energetic contribution that is independent of distance, $B \equiv \mu_C + u_C$. For the interaction $w = \beta(d/a)^{-p}$, we obtained the parameters $\beta = 6.25$ eV± 0.63 eV and $p = 3.6 \pm 0.05$. Therefore, in contrast to the case of DVs ($p = 2$), we find that the interactions between equivalent carbons that substitute Si atoms in the same dimer row is more short ranged, as indicated by the exponent value of $p = 3.6$. The reason for this difference between C atoms on the surface and DVs stems from considerations of symmetry of the atomic relaxations. Specifically, in the case of DVs, the relaxation occurs symmetrically on the two sides of the DV along the dimer row direction, and also in the direction perpendicular to it. In the case of first layer carbon atoms, there is no symmetry of the atomic displacements perpendicular to the dimer row, since the Si-C surface dimer is tilted. The reduced symmetry necessarily gives rise to nonvanishing higher-rank multipole moments [28], therefore generating exponents higher than $p = 3$ in Eq. (6).

The lack of symmetry in the direction perpendicular to the dimer row contributes to the anisotropy of the interactions that is generated by the (2×1) reconstruction. The anisotropic character of the C-C interaction is evidenced by the atomic displacements around a substitutional carbon. As depicted in Fig. 2(a), the absolute magnitude of the displacement vectors [computed with respect to the reconstructed Si(001) surface] shows severe confinement around the dimer row to which the carbon defect belongs. The strength of this confinement, and thus the direction dependence of the interactions, will decrease when the substitutional carbons are placed in deeper surface layers. This can be seen in Fig. 2(b), which shows the magnitude of displacements for the case of carbon substituting a Si atom in the fourth layer, below a dimer (α site). The substitutional α-site carbons have been reported to favor the creation of DV on the surface [4,11,19]. It is therefore of interest to calculate the interactions between C atoms and dimer vacancies, an issue which we address next.
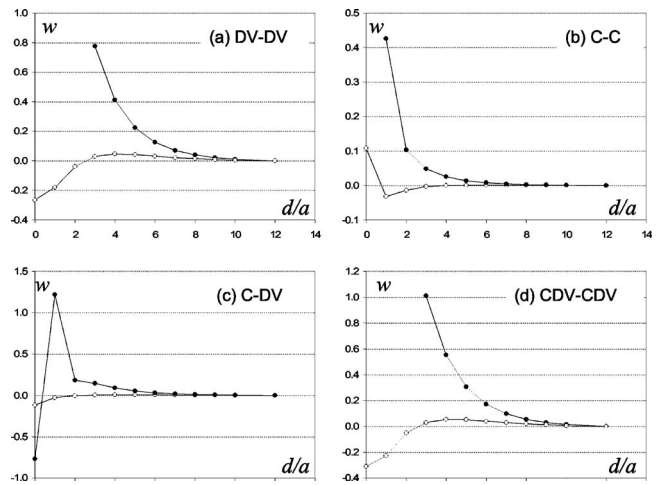
4   C Atoms and Dimer Vacancies on Si(001)

4.1   C-DV Interactions. Following the procedure outlined in Sec. 2, we evaluate, in turn, the interactions between different types of defects that lie either in the same dimer row or in adjacent dimer rows. As shown in previous studies (e.g., [21,24,26]), two DVs repel strongly when they belong to the same dimer row,
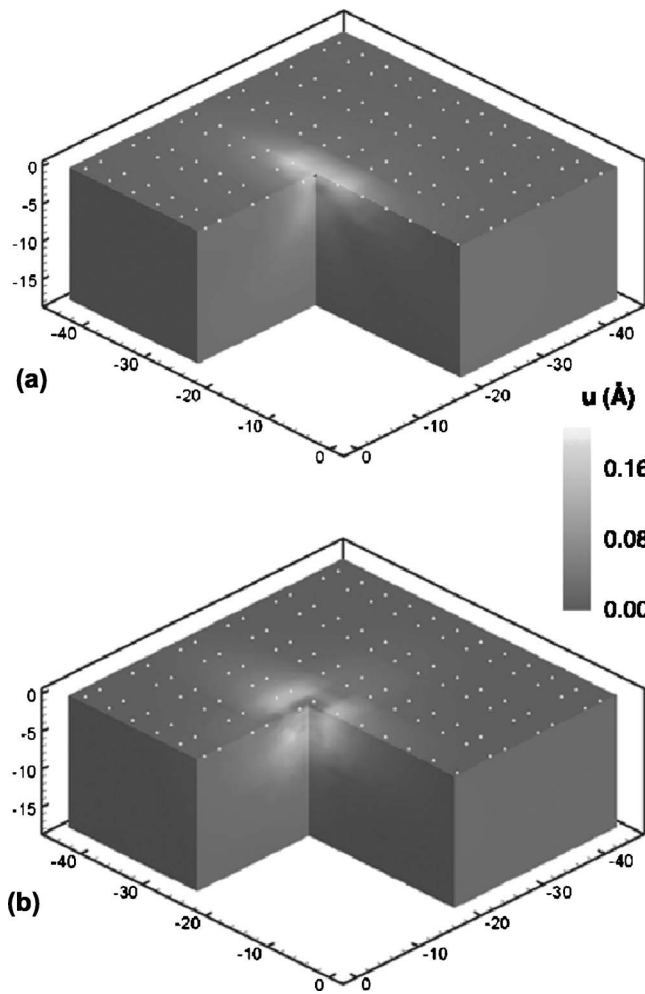
Fig. 2 Contour plots of the magnitudes (in angstroms) of atomic displacements caused by a substitutional carbon atom in the first layer (*a*), and in a fourth layer α-site (*b*). The displacements are computed with respect to the defect-free Si(001) surface. The locations of the surface atoms are shown by the small dots, to help visualize the (2×1) reconstruction. A quarter of the slab has been blanked in order to show the displacement contours in different planes.

Fig. 3 Interaction energies *w* (in electron-volts) between (*a*) two DVs, (*b*) two C atoms, (*c*) one C atom and one DV, and (*d*) two CDV complexes plotted as functions of their separation *d* measured along the dimer row direction. The interactions are sizeable only when the two entities lie in the same dimer row (solid circles) or in adjacent dimer rows (open circles). The substitutional carbon atoms considered here belong to the α sites in the fourth layer. The distance *d* (horizontal axis) is expressed as integer multiples of the dimer spacing $a=3.84$ Å.

but experience a weak, short-range attraction when they lie in adjacent rows. The strong repulsion of the DVs in the same dimer row is due to the fact that the atoms between the vacancies are pulled in opposite directions (toward each of the DVs), and their relaxation is hindered [24]. The attraction between the two DVs in adjacent rows, at their closest separation, is estimated at −0.27 eV using the Tersoff potentials [26]. The interaction between the DVs in adjacent dimer rows remains attractive until their separation exceeds three dimer spacings [Fig. 3(*a*)], after which it becomes repulsive.

When two C atoms in the fourth layer and the same dimer row are considered, we find that interaction is repulsive as expected from considerations of strain relaxation. For two C atoms that are placed in the fourth layer in adjacent dimer rows, we find a weak attraction when the separation along the dimer row is 1 to 3 dimer spacings [refer to Fig. 3(*b*)]. We note that, in contrast to the case of two DVs, the interactions between two C atoms decay faster as the distance between them (measured along the dimer rows) increases. We now turn to describing the interactions between one C atom and one DV. Recent experimental [4,11] and theoretical [19] reports are in agreement regarding the fact that the C atoms bind to the dimer vacancy, with the most favorable position being right

underneath the missing dimer, as shown in Fig. 1. For this reason we consider here only C atoms in the fourth layer, as they have been observed to create the most stable CDV complexes. The binding energy that we have obtained at the level of empirical potentials is −0.766 eV [refer to Fig. 3(*c*)]. This value is in quite good agreement with the attractive energy of −0.68 eV obtained from density functional calculations [19]. When the C atom and the DV belong to adjacent dimer rows, we find a much weaker attraction of only −0.118 eV at their minimum relative separation. In all other cases, the interaction between a fourth layer C atom and a DV is either very weak or repulsive, as shown in Fig. 3(*c*).

When the C atom and the DV bind together, they form complexes (named here CDVs) that are very stable energetically and have a reduced mobility compared to the mobility of their individual components. The interactions between CDV complexes are very similar to the interactions between two DVs, i.e., repulsive in the same dimer row and short-range attractive in adjacent dimer rows [Fig. 3(*d*)]. The features of the CDV-CDV interactions are mainly determined by those of the DV-DV interactions, since they are stronger than both the C-C and the C-DV interactions for most of the relevant separations *d* (refer to Fig. 3). The binding energy of two CDV complexes that lie in adjacent dimer rows is −0.31 eV, slightly stronger than that corresponding to two pure DVs [26].

The general characteristics of the interactions described above are consistent with recent experiments [4,11]. First, in experiments reported in Ref. [4] the number of C atoms and the number of DVs are approximately equal, which lends support to the idea of forming CDV complexes. Second, the complexes have been observed to align with one another [4,11], forming linear structures that are similar to those observed in the (2×*N*) reconstructions of the Ge/Si(001) surface [12,13]. There are three main features of the interactions computed above that explain some of the observations [4,11] in the low-coverage regime where our calculations are relevant: (a) the attractive interaction between a C atom and a DV, (b) the attraction between two CDV complexes that lie in adjacent dimer rows, and (c) the long-range repulsive interactions that occur in most other situations (refer to Fig. 3).

4.2 Monte Carlo Simulations. To verify that the interactions computed with the Tersoff potentials (Fig. 3) are able to capture
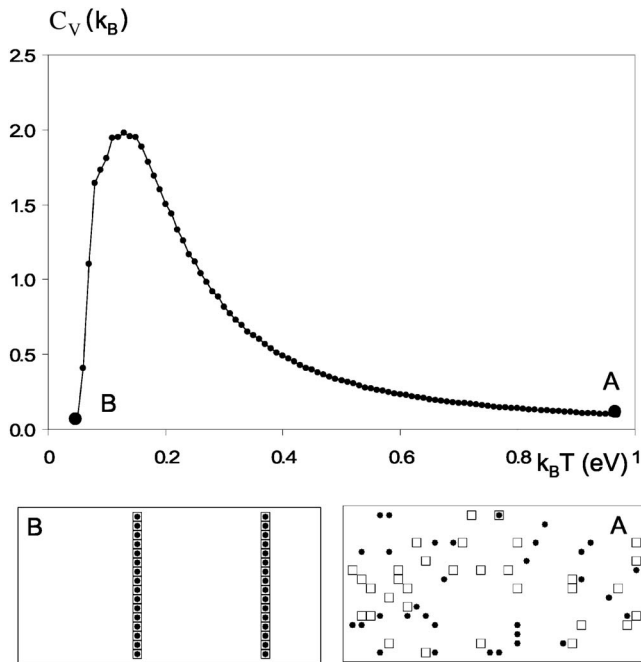
Fig. 4 Heat capacity of a model system with 32 carbon atoms, calculated during a slow cooling from $T=0.95$ eV/k_B down to $T=0.05$ eV/k_B. The initial and final configurations (A and B, respectively) show that the carbon atoms (solid circles) form complexes with the DVs (empty squares), which assemble into long linear structures during annealing.

the main physics of self-assembled lines on C/Si(001), we now compare predictions based on these interactions with recent experimental results in the low-coverage limit [4,11]. We have set up a thermodynamic Monte Carlo simulation of the incorporated C atoms and DVs on the surface. The simulation is lattice based, where the DVs and C atoms can only perform jumps on the nodes of a two-dimensional grid. The following set of simplified rules defines the course of the simulations:

(1) The substitutional carbon atoms can only occupy the α sites in the fourth layer.
(2) Configurations with two DVs (or two CDVs) that are separated by one (3.84 Å) or two lattice spacings (7.68 Å) in the same dimer row are forbidden.
(3) The interactions between defects are given by the values in Fig. 3, and are negligible if the two defects involved are not in the same row or adjacent rows.
(4) The interactions between one C atom and one CDV complex are taken to be same as the interactions between two C atoms; similarly, the interactions between one DV and one CDV complex are set to the interactions between two DVs.

Based on this set of rules, we have performed simulations for systems of various sizes. The typical simulation is started at high temperatures ($T_{max} \approx 1$ eV/k_B, where k_B is the Boltzmann's constant), because the relevant energy scale is dictated by the binding between a C atom and a DV, -0.766 eV. At the highest temperature, we have performed a number of 5000 equilibration passes, followed by 50,000 accumulation passes used in computing thermodynamic quantities such as energy and heat capacity. After the accumulation passes performed at T_{max}, the temperature is lowered in steps of $\Delta T = 0.01$ eV/k_B, and for each temperature the equilibration-accumulation sequence is repeated. The cooling is stopped when the temperature reaches $T_{min}=0.05$ eV/k_B.

We have analyzed the heat capacity of the system during cooling, which is plotted in Fig. 4 for a system of 32 carbon atoms and

an equal number of DVs. The peak of the heat capacity plot indicates a phase transition corresponding to the formation and ordering of CDV complexes. As shown in the lower panels of Fig. 4, the system starts out with a random configuration of DVs and C atoms, and forms evenly spaced straight lines of CDV complexes at end of the cooling procedure. This finding is consistent with the work of Kim and coworkers who reported evidence of CDV lines on C/Si(001) [4,11]. The main difference between the simulation results shown in Fig. 4 and the experimental work of Kim et al. concerns the length and the shape of the vacancy lines, which have been found to be jagged and not very long [4,11]. This morphological discrepancy between the simulation results and the experimental observations is largely due to rule (1) listed above, which restricts the configuration space that the carbon atoms can explore: Therefore, during a careful simulated annealing, it becomes much more likely for the carbon atoms to find the dimer vacancies and bind with them, since their motion is confined to the fourth layer. On the other hand, in experiments there is no such preset confinement for the C atoms, which have a much larger number of configurations to explore. The larger dimension of the configuration space of the carbon atoms and the realistic annealing schedules performed in laboratory are the probable reasons why the aspect of the vacancy lines is jagged rather than straight. We note that, in order to obtain a jagged aspect of the CDV lines we can simply use fewer Monte Carlo passes at each temperature, thus not allowing the system to reach equilibrium ("freeze in").

These results are consistent with experiments, so we conclude that the Tersoff potentials are sufficient to qualitatively capture the energetics of substitutional carbons and dimer vacancies. Furthermore, since the simulation does not address kinetic effects in any way, the agreement with experiments may suggest that the self-assembly of CDV lines on C/Si(001) is mainly governed by energetics rather than kinetics, although the latter does have a contribution in limiting the length of the CDV lines. Maintaining the focus on the thermodynamically stable morphologies, we will now describe an energetic mechanism that determines the spacing between the CDV lines of the $(2 \times N)$ structure.

4.3 Formation Energy and Repulsive Interactions of CDV Lines. The $(2 \times N)$ reconstruction is a structural pattern on the (001) surface of Si, characterized by the periodic lengths $L_x=Na$ and $L_y=2a$, where N is a positive integer and $a=3.84$ Å is the lattice constant of the unreconstructed Si(001) surface. This reconstruction is obtained by eliminating every Nth dimer from each dimer row, such that the dimer vacancies created in this manner are in registry with one another and form straight lines perpendicular to the dimer rows. To lower the number of dangling bonds at the surface, the second-layer atoms below the dimer vacancy rebond such that they are fully coordinated, at the cost of introducing some surface stress [20]. At low amounts of incorporated carbon, the dimer vacancies are further stabilized by C atoms incorporated in the fourth layer below the missing dimer (Fig. 1). In this subsection we focus on the general features of the energetics of the $(2 \times N)$ surface, then make connection with the case of CDV lines. We partition the surface energy into a contribution from the (2×1) surface and a contribution from the vacancy lines

$$\gamma_{2 \times N} = \gamma_0 + \frac{\lambda}{L_x}, \qquad (7)$$

where $\gamma_{2 \times N}=(E-N_{Si}\mu_{Si}-\mu_C)/A$ denotes the surface energy of $(2 \times N)$ structure and λ is the energy of vacancy lines per unit length. Equation (7) defines the energy per unit length λ of the CDV lines as an excess energy with respect to the defect-free (2×1) surface. We note that λ includes the formation energy of the lines, as well as their elastic interactions. Based on prior results on the vacancy lines on Ge/Si(001) [26], we expect the interactions

to be inversely proportional with the square of the line separation, so we write line energy λ as

$$\lambda = \Lambda + \frac{\pi^2}{6} \frac{G}{L_x^2}, \qquad (8)$$

where Λ is the formation energy and G is the strength of the elastic repulsion. The numerical factor $\pi^2/6$ arises since we treat a periodic array of CDV lines, rather than two isolated ones. Substituting Eq. (8) in Eq. (7), we can write the surface energy of the $(2 \times N)$ reconstruction as a function of N

$$\gamma_{2 \times N} = \gamma_0 + \frac{\Lambda}{Na} + \frac{\pi^2}{6} \frac{G}{N^3 a^3}. \qquad (9)$$

Equation (9) indicates that there exists a minimum of the surface energy $\gamma_{2 \times N}$ if the formation energy Λ is negative. Using 50 Å thick $(2 \times N)$ slabs with $6 \leqslant N \leqslant 24$, we computed the surface energy $\gamma_{2 \times N}$ and fit it to Eq. (9) in order to extract the formation energy and repulsion strength of the CDV lines. For a value of the carbon chemical potential equal to the cohesive energy in diamond ($\mu_C = -7.37$ eV [15]), we found that $\Lambda = -45$ meV/Å and $G = 20.38$ eV Å. Since the formation energy is negative, we therefore conclude that the $(2 \times N)$ reconstruction is determined by the competition between the (negative) formation energy of the CDV lines and their (positive) elastic repulsion. This is the same energetic mechanism that we evidenced for the case of self-organized vacancy lines on Ge/Si(001) [26].

With the above values for Λ and G, the direct minimization of Eq. (9) yields an optimal value of $N^* = (\pi/a)\sqrt{G/(-2\Lambda)} = 12.3$, in agreement with location ($N = 12$) of the minimum of $\gamma_{2 \times N}$ determined from simulations. The position of the surface energy minimum depends on the choice of μ_C. Since $\gamma_{2 \times N} = (E - N_{Si}\mu_{Si} - \mu_C)/A$, a finite variation $\delta\mu_C$ of the chemical potential of carbon determines a finite variation

$$\delta\gamma_{2 \times N} = -\frac{\delta\mu_C}{2Na^2}. \qquad (10)$$

By taking the variation of Eq. (9) caused by μ_C, and comparing it with Eq. (10), we find that the change $\delta\mu_C$ determines a change in the formation energy $\delta\Lambda = -\delta\mu_C/2a$ but leaves the repulsion strength G unaltered ($\delta G = 0$). We therefore note that an increase in chemical potential of carbon ($\delta\mu_C > 0$) enhances the tendency of the system to form CDV lines. Since the chemical potential μ_C is not directly tuned in experiments, this trend may be useful for further investigations of the dissociation of organic molecules at the surface in the low coverage regime. Knowing that the coverage θ_C at which CDV lines are present is $0.02 \text{ ML} < \theta_C < 0.05 \text{ ML}$ [4], we can estimate the range of the chemical potential μ_C for which the $(2 \times N)$ features can be observed. The carbon coverage θ_C is related to the optimal (or in experiments, with the *average*) line spacing N^* through $\theta_C = 1/2N^*$. As mentioned, this spacing is given by $N^* = (\pi/a)\sqrt{G/(-2\Lambda)}$, and is therefore controlled by the chemical potential μ_C via the formation energy Λ. The variation of N^* with μ_C can be observed from graphs of the surface energy $\gamma_{2 \times N}$ plotted for different values of μ_C (refer to Fig. 5). As the C chemical potential is increased from -7.63 eV to -7.00 eV, the minimum of the surface energy becomes more pronounced and moves toward lower values of the CDV line spacing. The position of the optimum spacing N^* is shown as a function of μ_C in Fig. 6. For relevant carbon coverages ($0.02 \text{ ML} < \theta_C < 0.05 \text{ ML}$), the line spacing varies in the range $10 < N^* < 25$, which corresponds to the μ_C interval $-7.63 \text{ eV} < \mu_C < -7.19 \text{ eV}$, as shown in Fig. 6.

5 Summary

In this article we have touched upon the problem of interacting defects on reconstructed semiconductor surfaces using substitu-
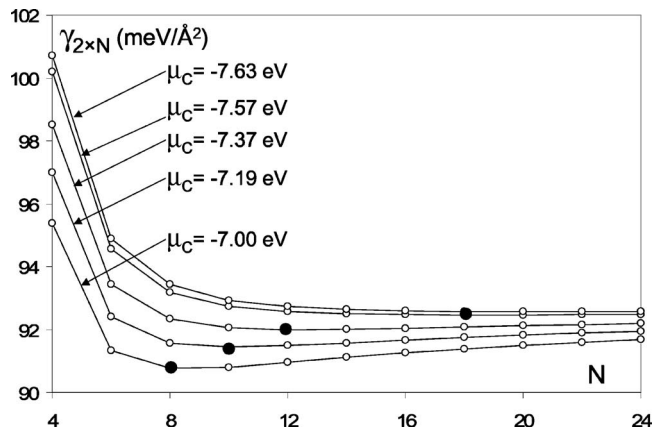
Fig. 5 Surface energy of the $(2 \times N)$ reconstruction on C/Si(001) as a function of N, plotted for different values of the chemical potential μ_C. The solid dots show the locations N^* of the surface energy minima, which move towards smaller values with increasing μ_C.

tional carbon atoms on Si(001)-(2×1) as an example. The reconstruction of this surface gives rise to highly anisotropic interactions whose strengths also depend on the position of the carbon atoms with respect to the silicon dimers on the surface. While the anisotropic character of interacting defects has previously been studied (see, for example, the case of adatoms on metal surfaces [29]), the source of anisotropy under consideration was the direction dependence of the elastic constants, rather than the atomic-scale features of a reconstructed surface. Here we showed evidence of how the reconstruction of Si(001) can affect the interactions of substitutional C defects; further efforts aimed at elucidating the relation between the defect structure and the interaction energy are underway.

Motivated by recent experiments reporting that incorporation of carbon favors the formation of dimer vacancies on the Si(001), we have also calculated the interaction between carbon atoms and dimer vacancies at the level of Tersoff potentials [15–17]. Our results are consistent with the observation [4] of CDV lines on Si(001). The self-organization of these lines is determined by a mechanism similar to that responsible for the formation of vacancy lines on Ge-covered Si(001). This mechanism is based on the attraction between two CDV complexes in adjacent dimer
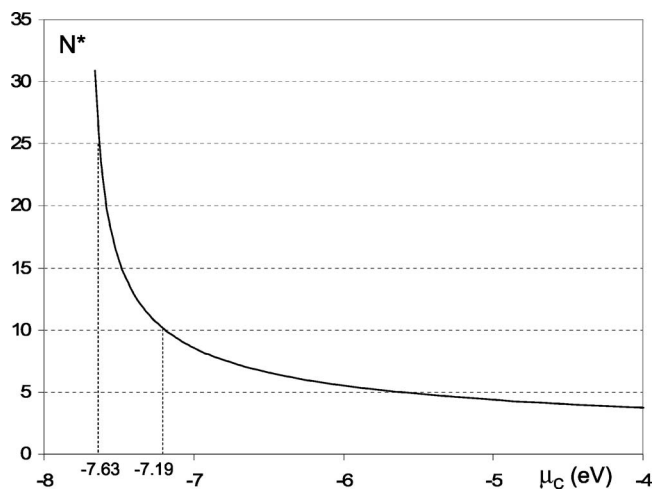

Fig. 6 Optimal value N^* as a function of the chemical potential μ_C. The chemical potential range that corresponds to experimentally relevant carbon coverages is $-7.63 \text{ eV} < \mu_C < -7.19 \text{ eV}$.

rows, and repulsive interactions between CDVs situated in the same dimer row: The former interaction leads to the formation of the CDV lines by bonding complexes in adjacent dimer rows, while the latter helps maintain a constant average spacing between these lines. By use of simple thermodynamic simulations, we have verified that the interactions computed with Tersoff potentials are physically relevant, as the simulations are in agreement with the recent experimental observations [4,11]. The numerical value of the binding energy of a CDV complex (-0.766 eV, computed at the level of Tersoff potentials) is reasonably close to the -0.68 eV value predicted by density functional calculations [19]. Finally, we have discussed the energetics of the $(2 \times N)$ reconstruction and showed that the self-assembly of CDV lines may be understood as a competition between the formation energy of the lines and their elastic repulsion. Pending an increase in the available computational power and methodologies, the results of this article may warrant future studies using higher-level total-energy methods such as tight-binding or density functional calculations. The use of such methods is expected to bring quantitative improvements of the energetic properties computed here. Furthermore, higher-level methods can also address other important aspects of the self-assembly of vacancies, such as the energy barriers associated with the creation and diffusion of carbon atoms and vacancies on Si(001).

Acknowledgments

References

[1] Houghton, D. C., Aers, G. C., Rowell, N. L., Brunner, K., Winter, W., and Eberl, K., 1997, "Band Alignment in $Si_{1-y}C_y$/Si(001) and $Si_{1-x}Ge_x$/$Si_{1-y}C_y$/Si(001) Quantum Wells by Photoluminescence under Applied [100] and [110] Uniaxial Stress," Phys. Rev. Lett., **78**, pp. 2441–2444.

[2] Ohfuti, M., Awano, Y., and Yokoyama, N., 1999, "First-Principles Study on the Origin of Band-Gap Reduction in Si-Lattice Matched $Si_{1-x-y}Ge_xC_y$," Phys. Rev. B, **60**, pp. 15515–15518.

[3] See, for example, Osten, H. J., Lippert, G., Liu, G. P., and Kruger, D., 2000, "Influence of Carbon Incorporation on Dopant Surface Segregation in Molecular-Beam Epitaxial Growth of Silicon," Appl. Phys. Lett., **77**, pp. 2000–2002; Osten, H. J., Kim, M., Pressel, K., and Zaumseil, P., 1996, "Substitutional Versus Interstitial Carbon Incorporation During Pseudomorphic Growth of $Si_{1y}C_y$ on Si(001)," J. Appl. Phys., **80**, pp. 6711–6715.

[4] Kim, W., Kim, H., Lee, G., and Koo, J.-Y., 2002, "Initial Stage of Carbon Incorporation into Si(001) and One-Dimensional Ordering of Embedded Carbon," Phys. Rev. Lett., **89**, pp. 106102–106102.

[5] Kelires, P. C., 1997, "Parity Effect in Ground State Energies of Ultrasmall Superconducting Grains," Phys. Rev. Lett., **78**, pp. 3749–3752.

[6] Ramamoorthy, M., Briggs, E. L., and Bernholc, J., 1998, "Chemical Trends in Impurity Incorporation into Si(100)," Phys. Rev. Lett., **81**, pp. 1642–1645.

[7] Liu, C. L., Borucki, L. J., Merchant, T., Stocker, M., and Korkin, A., 2000, "Ab Initio Investigation of C Incorporation Mechanisms on Si(001)," Appl. Phys. Lett., **76**, pp. 885–887.

[8] Sonnet, P., Stauffer, L., Selloni, A., De Vita, A., Car, R., Simon, L., Stoffel, M., and Kubler, L., 2000, "Energetics of Surface and Subsurface Carbon Incorporation in Si(100)," Phys. Rev. B, **62**, pp. 6881–6884.

[9] Leifeld, O., Grützmacher, D., Müller, B., Kern, K., Kaxiras, E., and Kelires, P. C., 1999, "Dimer Pairing on the C-Alloyed Si(001) Surface," Phys. Rev. Lett., **82**, pp. 972–975.

[10] Remediakis, I. N., Guedj, C., Kelires, P. C., Grützmacher, D., and Kaxiras, E., 2004, "Modeling of the Carbon-Rich $c(4 \times 4)$ Reconstruction on Si(100)," Surf. Sci., **554**, pp. 90–102.

[11] Kim, W., Kim, H., Lee, G., You, S.-Y., Hong, Y.-K., and Koo, J.-Y., 2002, "Formation of Atomically Flat Si(001) Surface with Incorporated Carbon," Surf. Sci., **516**, pp. L553–L556.

[12] Mo, Y. W., and Lagally, M. G., 1991, "Scanning Tunneling Microscopy Studies of the Growth Process of Ge on Si(001)," J. Cryst. Growth, **111**, pp. 876–881.

[13] Köhler, U., Jusko, O., Müller, B., Horn-von Hoegen, M., and Pook, M., 1992, "Layer-by-Layer Growth of Germanium on Si(100): Strain-Induced Morphology and the Influence of Surfactants," Ultramicroscopy, **42–44**, pp. 832–837.

[14] Kim, H., Kim W., Lee, G., and Koo, J,-Y., 2005, "Two Dimensional Carbon Incorporation and Structure of Si(001)-$c(4 \times 4)$," Phys. Rev. Lett., **94**, pp. 076102–076102.

[15] Tersoff, J., 1989, "Modeling Solid-State Chemistry: Interatomic Potentials for Multicomponent Systems," Phys. Rev. B, **39**, pp. 5566–5568. Also see the related erratum, Tersoff, J., Phys. Rev. B, **41**, p. 3248.

[16] Tersoff, J., 1990, "Carbon Defects and Defect Reactions in Silicon," Phys. Rev. Lett., **64**, pp. 1757–1760.

[17] Tersoff, J., 1994, "Chemical Order in Amorphous Silicon Carbide," Phys. Rev. B, **49**, pp. 16349–16352.

[18] Kelires, P. C., 1995, "Monte Carlo Studies of Ternary Semiconductor Alloys: Application to the $Si_{1-x-y}Ge_xC_y$ System," Phys. Rev. Lett., **75**, pp. 1114–1117; Kelires, P. C., 1996, "Microstructural and Elastic Properties of Silicon-Germanium-Carbon Alloys," Appl. Surf. Sci., **102**, pp. 12–16.

[19] Sonnet, Ph., Stauffer, L., Selloni, A., and Kelires, P. C., 2003, "Defect-Mediated Carbon Incorporation in the Si(001) Surface: Role of Stress and Carbon-Defect Interactions," Surf. Sci., **544**, pp. 277–284.

[20] Pandey, K. C., *Proceedings of the 17th International Conference on Physics of Semiconductors*, Chadi, D. J., and Harrison W. A., eds., 1985, Springer-Verlag, NY.

[21] Chen, X., Wu, F., Zhang, Z., and Lagally, M. G., 1994, "Vacancy-Vacancy Interaction on Ge-Covered Si(001)," Phys. Rev. Lett., **73**, pp. 850–853.

[22] Chang, C. S., Huang, Y. M., Chen, C. C., and Tsong, T. T., 1996, "Anisotropic Interaction of Ag-Induced Missing Dimer Vacancies on Si(001) Surfaces," Surf. Sci., **367**, pp. L8–L12.

[23] Zandvliet, H. J. W., Louwsma, H. K., Hegeman, P. E., and Poelsema, B., 1995, "Energetics of Ni-Induced Vacancy Line Defects on Si(001)," Phys. Rev. Lett., **75**, pp. 3890–3893.

[24] Weakliem, P. C., Zhang, Z., and Metiu, H., 1995, "Missing Dimer Vacancies Ordering on the Si(100) Surface," Surf. Sci., **336**, pp. 303–313.

[25] Natori, A., Nishiyama, R., and Yasunaga, H., 1997, "Stability of Ordered Missing-Dimer Structures and the Ordering Dynamics on Si(001)," Surf. Sci., **397**, pp. 71–83.

[26] Ciobanu, C. V., Tambe, D. T., and Shenoy, V. B., 2004, "Comparative Study of Dimer-Vacancies and Dimer-Vacancy Lines on Si(001) and Ge(001)," Surf. Sci., **556**, pp. 171–183.

[27] Marchenko, V. I., and Parshin, A. Ya., 1980, "On the Elastic Properties of Crystal Surfaces," Sov. Phys. JETP, **52**, pp. 129–131.

[28] Teodosiu, C., 1982, *Elastic Models of Crystal Defects*, Springer-Verlag, Berlin.

[29] Shilkrot, L. E., and Srolovitz, D. J., 1997, "Anisotropic Elastic Analysis and Atomistic Simulation of Adatom-Adatom Interactions on Solid Surfaces," J. Mech. Phys. Solids, **45**, pp. 1861–1873.